

# The Blairgowrie magnetic anomaly and its interpretation using simplex optimisation

Colin G. Farquharson and Roy Thompson

**ABSTRACT:** The large magnetic anomaly which runs along the Highland Boundary Fault of Scotland immediately to the NW of Blairgowrie has been studied by both a ground-based magnetic survey and a palaeomagnetic investigation. A newly developed optimisation program, making use of a simplex algorithm, was used to model the long wavelength component of this effectively two-dimensional anomaly. The consequent model consists of a vertical, rectangular body, 3 km wide and 13 km deep, whose top surface is 2 km below ground level, with a magnetisation directed vertically downwards. The composition of this body is most likely to be that of an ultra-basic, metamorphic complex which has been brought up to its present position between two of the many near-vertical faults in the area. The medium wavelength structure of the anomaly was modelled using the common technique of trial and error, and can be interpreted in terms of a pair of Devonian andesitic lavas and a small extension of the main ultrabasic block. Subsequent palaeomagnetic remanence measurements confirmed that the magnetisation of the two lavas recorded a Devonian polarity reversal. The magnetisation of the ultrabasics is directed vertically downwards, exactly as deduced from the earlier modelling work.



**KEY WORDS:** total magnetic field, magnetised prisms, palaeomagnetism, serpentinite, Highland Boundary Fault zone.

## 1. Introduction

The Blairgowrie magnetic anomaly is a noticeable feature of the aeromagnetic map of Scotland (BGS 1981), with an amplitude of 600 nT surpassed only by anomalies associated with the igneous complexes of Mull and Skye. This large total field anomaly, with its maximum development immediately to the NW of Blairgowrie, appears to lie along the line of the Highland Boundary Fault separating Dalradian metamorphic rocks to the north from the Old Red Sandstone to the south. However, in the vicinity of Blairgowrie, the junction is complicated, with numerous faults forming a wide fault zone. The Blairgowrie magnetic anomaly could be associated with this complex faulted region. A ground-based survey of the total magnetic field and a palaeomagnetic study have been carried out to provide an indication of the nature of the magnetic anomaly source, and to shed some light on the structure and deep geology of the area.

In addition, a mathematical optimisation procedure has been developed to improve existing techniques for modelling the total field magnetic anomaly produced by a uniformly magnetised, two-dimensional body. It is hoped that this will make interpretation of such anomalies much less time-consuming.

## 2. The Blairgowrie magnetic anomaly and its geological setting

The Blairgowrie aeromagnetic anomaly has an elongated shape, running in a NE–SW direction for over 40 km (Fig. 1), and has an amplitude of 600 nT as observed at a height of 300 m above ground level. By comparing Figure 1a and 1b, the Blairgowrie magnetic anomaly is seen to coincide

almost exactly with a complex section of the Highland Boundary Fault Zone. This major fault zone separates the Grampian Highlands from the Midland Valley of Scotland. To the N and W of the Highland Boundary Fault Zone are metamorphic rocks of the Dalradian series, while to the S and E there are rocks of the Old Red Sandstone series. The geology immediately NW of Blairgowrie is rather complicated, with a succession of faulted blocks, outcrops of serpentinite and several Devonian andesitic lavas. The surface geology is summarised in Figure 2.

## 3. Total magnetic field measurements and data manipulation

The anomaly was investigated by measuring the total magnetic field along a profile perpendicular to the axis passing through the town of Blairgowrie. The linear nature of the anomaly means that two-dimensional modelling techniques can be used to interpret the profile.

Measurements were made of the total field using a Geometrics G856AX proton precession magnetometer. It was impossible to follow a direct route across the Blairgowrie anomaly. Instead, survey lines were chosen to follow the roads in the area, although, whenever possible, readings were taken in fields at 10–20 m from the roads in order to avoid the magnetic effects of vehicles, fences and drains. The main profile was constructed by combining the various survey lines, each a few kilometres in length. Individual survey lines are shown on the map of Figure 2. A long profile was measured to determine the regional field accurately and a spacing of 100 m between measurements chosen as appropriate for investigation of this 8 km-wide anomaly. This resulted in over 200 measurements along the 21 km profile.

Repeated measurements at a base station in Blairgowrie [NO 177 455] allowed a correction for the daily variation of the geomagnetic field to be made. It was found that a simple linear approximation for the time variation of the main field between base station readings was adequate since the observed variation with time of order 10 nT was small compared with the 1000 nT amplitude of the anomaly.

The corrected values of the magnetic anomaly along lines 1–5 were projected onto the single straight line labelled AB in Figure 2 by plotting each measurement at the point where the straight line passing through the measurement location and running perpendicular to the profile AB intersected AB. The resulting total field magnetic anomaly along the line AB is plotted in Figure 3.

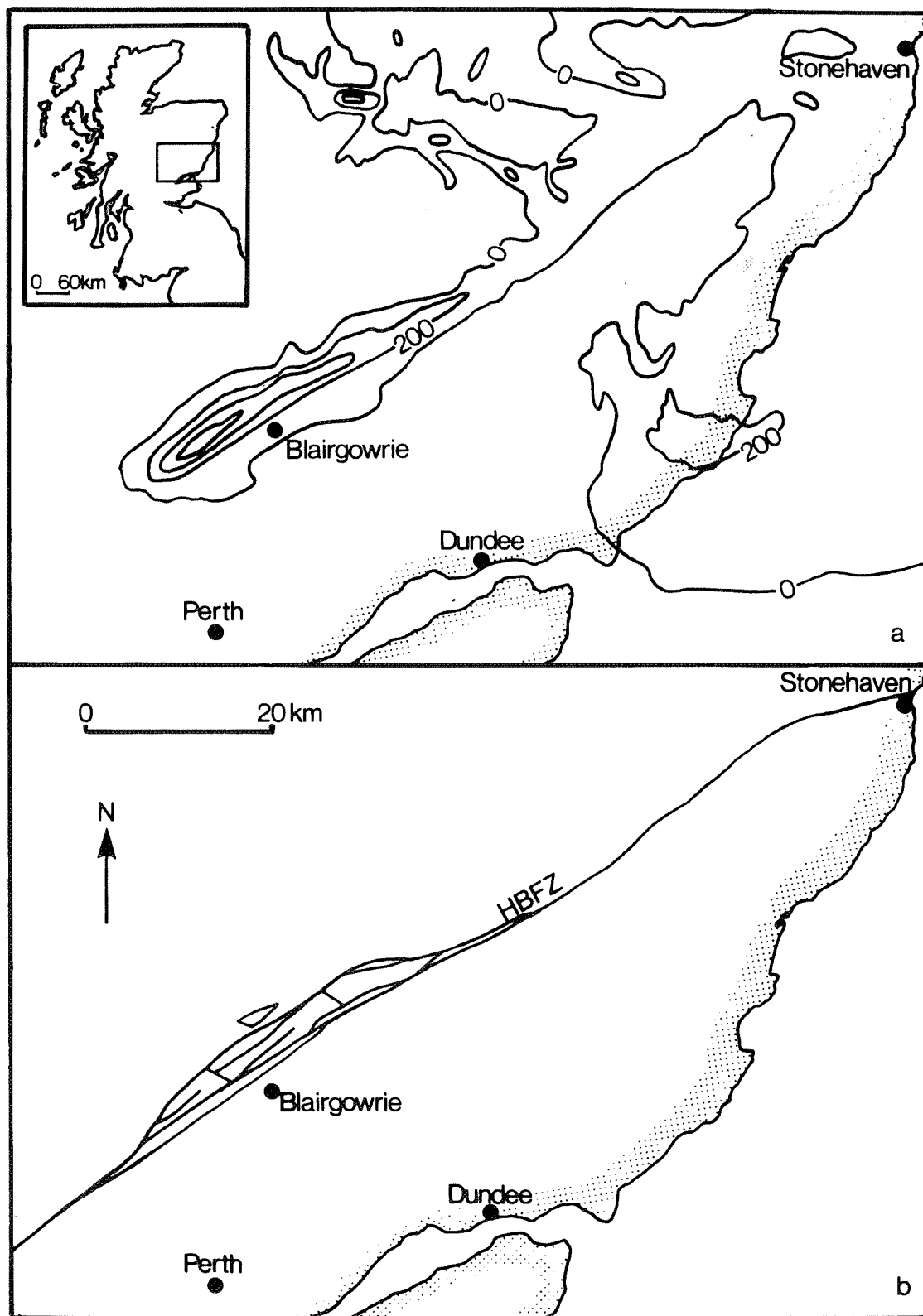


**Figure 1** (a) Aeromagnetic map of the Strathmore area showing the large, elongated Blairgowrie anomaly. The contour interval is 200 nT. (b) Tectonic map of the same area as Figure 1a showing the Highland Boundary Fault Zone (HBFZ), simplified from Armstrong and Paterson (1970). Inset shows location within Scotland.

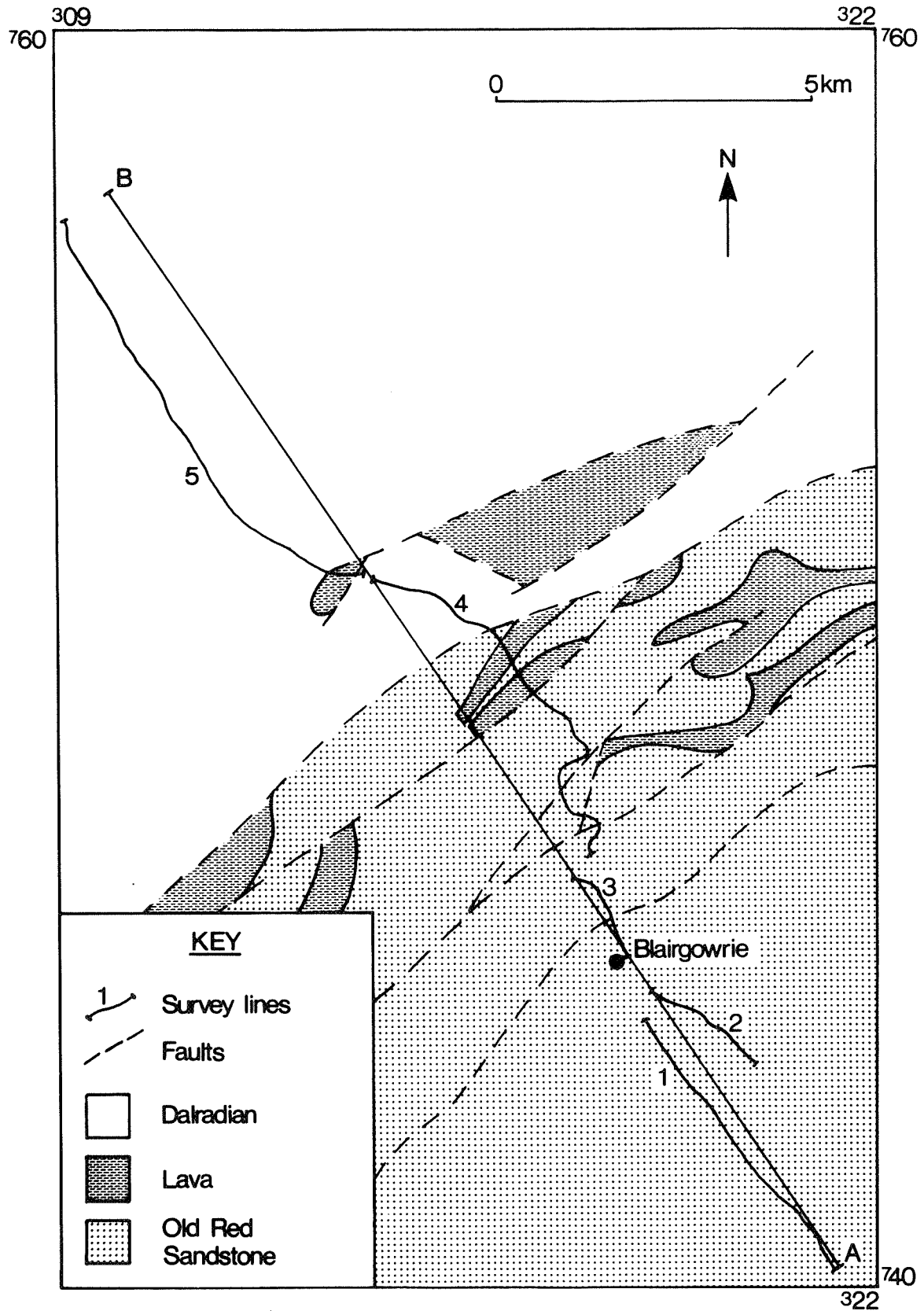


**Figure 2** Simplified geological map of the area around Blairgowrie showing the Devonian lavas, and illustrating the complexity of the Highland Boundary Fault Zone in this region. The survey lines along which the measurements were made are also shown. The line AB is the straight line onto which these measurements were projected before modelling. The numbers at the corners of the map refer to the Ordnance Survey National Grid.

#### 4. Magnetic anomaly interpretation

Because of the elongated nature of the Blairgowrie anomaly, the magnetic profile could justifiably be interpreted in terms of two-dimensional bodies. However, as the profile in Figure 3 indicates, the magnetic anomaly is very complex, with considerable short wavelength structures which do not appear on the aeromagnetic map. As a first step in interpretation it was assumed that these shorter wavelength features were superimposed upon an anomaly produced by a single magnetised body at a depth of several kilometres.

The most common method of interpreting geophysical total magnetic field anomalies is by trial and error modelling. Using this approach, the form of the subsurface body is guessed, along with its magnetisation characteristics. The theoretical magnetic field is then calculated at each observation site for comparison with the actual measurements. Inspection of type curves for bodies of simple shape (e.g. figs 8 and 12 in Parasnis 1979) or application of simple depth rules such as those of Smith (1959) can give a useful starting point for the calculations. Numerous other shapes

and magnetisations will then be tried until the fit between the modelled and the observed magnetic field is judged to be satisfactory. As part of the investigation of the deep magnetic source of the Blairgowrie anomaly we have developed a new computer-based optimisation procedure to automate the above modelling process. The method chosen to carry out this optimisation was based on the simplex algorithm of Nelder and Mead (1965).

##### 4.1. Simplex optimisation

The simplex method of Nelder and Mead for finding the minimum of a function need only be supplied with the values of the function to be minimised, and an initial estimate of the coordinates of the desired minimum, to set the procedure going. Gill *et al.* (1981) give a complete discussion of such optimisation techniques. The method of Nelder and Mead is straightforward and, although not the most efficient of methods, is robust and can be readily tailored to particular needs.

A simplex is a completely general body with a certain number of vertices. To minimise an object function of  $n$  variables, the Nelder and Mead algorithm uses a simplex with  $n + 1$  vertices. Each vertex lies on the hypersurface in the  $n$ -dimensional parameter space defined by the function to be minimised. The vertex with the largest value of the object function is then reflected through the centroid of the simplex to a position corresponding to a lower value of the function. This process then repeats itself, with the highest vertex being continually replaced by a point lower on the hypersurface. In this way, the simplex effectively rolls down the hypersurface until it finds itself straddling a minimum in the function, and so can go no further. The Nelder and Mead algorithm then makes the simplex contract, collapsing to a point in the bottom of the well corresponding to the minimum of the object function. Whether this is the desired global minimum, or just a local minimum, cannot, unfortunately, be determined without much effort. This difficulty remained a constant problem throughout this study, just as for any minimisation procedure. To implement the Nelder and Mead algorithm, the AMOEBA subroutine of Press *et al.* (1986) was used. A fully documented FORTRAN listing of the AMOEBA subroutine is given on pp. 292–3 of Press *et al.* (1986). The name of this subroutine arises from the way in which the simplex changes its shape and size as it rolls down the object surface in search of a minimum.

##### 4.2. Development of an automated search procedure

The optimisation problem was to minimise the residual sum of squares (RSS) between measured field values and the modelled field by varying the shape and magnetisation of a buried body. We represented this body by a four-sided prism of infinite extent in the direction perpendicular to the profile. Heiland (1940) gives a method of calculating the total field anomaly for any uniformly magnetised two-dimensional body from the effective magnetic charge density on each of its surfaces. Exact details of the method are given by Heiland (1940) in diagram 8-52 and equation 8-61e on pages 396 and 397 respectively. A FORTRAN program was written to calculate the total field anomaly of such a four-sided prism, execute the simplex optimisation and then display the measured values, the calculated anomaly and the optimised body shape. It involves some 1000 lines of FORTRAN code and can run on an IBM-PC. A flow diagram illustrating the structure of the program is given in Figure 4.

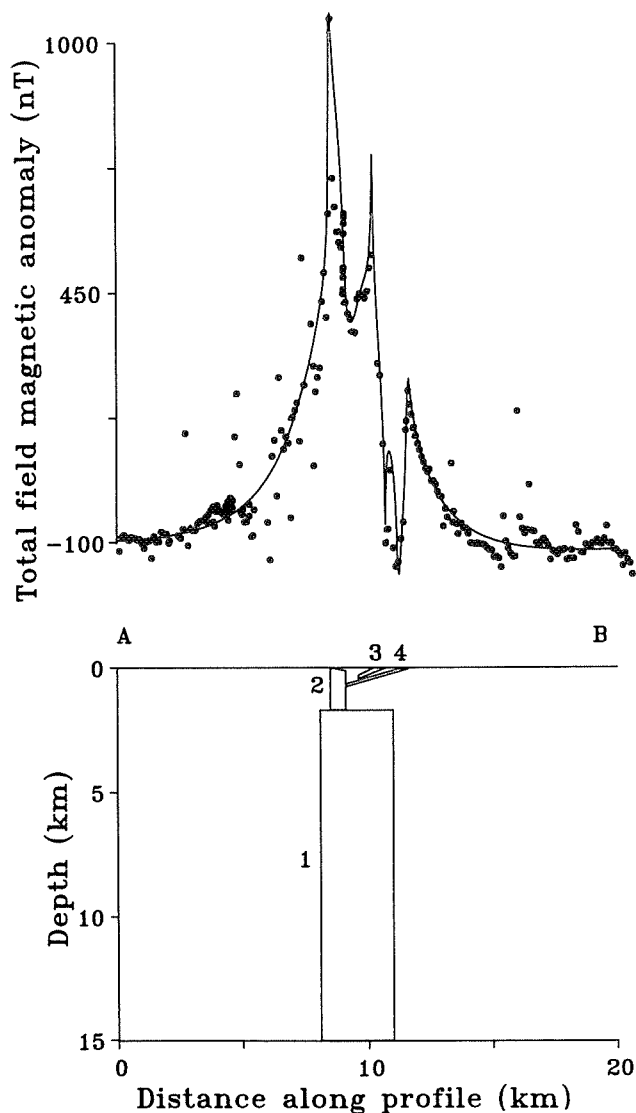


**Figure 3** The final model for the Blairgowrie magnetic anomaly. The direction and intensity of magnetisation of each of the four bodies are given in Table 1. The circles represent the actual measurements of the total field magnetic anomaly along the profile AB, and the continuous curve represents the calculated anomaly produced by the combination of the four magnetised bodies.

The program was tested both on synthetic anomalies, generated from bodies of known shape and magnetisation, and on some real magnetic datasets that had previously been examined by traditional trial and error modelling. This testing gave useful insights into the behaviour of the simplex optimisation. Firstly, the method often found a local minimum which was associated with an unacceptable model and from which the simplex could not extricate itself. As a consequence, a realistic starting position had to be chosen before any useful optimisation could begin. Secondly, early versions of the program contained no constraints on the possible shape of the prism. As Figure 5b shows, this produced some decidedly unorthodox cross-sectional shapes as the simplex rolled towards a minimum. Indeed, in some cases it even inverts the prism (cf. step 2 in Fig. 5b). A further aspect of early versions of the program is illustrated by step 4 in Figure 5b. The program consistently appears to want to lift three corners of the body up close to the ground surface in an attempt to model the finer structure of the data. The fourth corner is dispatched to a great depth in such a way that the magnetisation of the body is directed approximately towards this fourth corner. This means that the majority of the lower part of the magnetised body contributes very little towards the anomaly measured at the

surface. This can be understood by thinking in terms of the effective magnetic charge created on each surface of the two-dimensional body by its magnetisation. If the magnetisation points towards the deepest corner of the elongated shape the magnetisation will be almost parallel to the two sides meeting at the deepest corner. On account of this, only a very weak magnetic charge density is produced on these surfaces. This, combined with the thinness of the body, causes the equal and opposite contributions from the two sides to cancel each other and results in a negligible contribution to the measured anomaly.

The program was thus found to produce excellent mathematical solutions with great apparent physical insight, although (i) the solutions were of little geological value and (ii) the process was too frequently finding local minima rather than the desired global minimum.

In order to remedy these deficiencies we made three modifications to the program. First, as a means of addressing the lack of geological relevance of some of the prism shapes generated, the program was limited to fitting a dyke-shaped body, with horizontal top and bottom surfaces. This meant that the shapes which the final version of the program produced were much more like the traditional type of bodies used to model magnetic anomalies, as is shown in

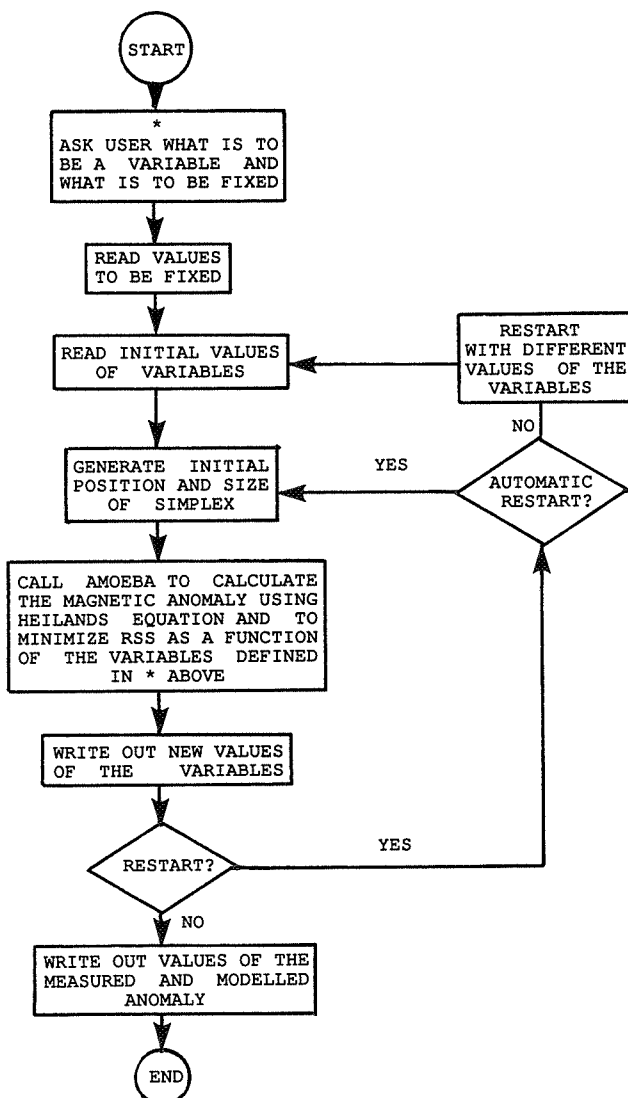


Figure 4 Flow diagram illustrating the structure of the optimisation program.

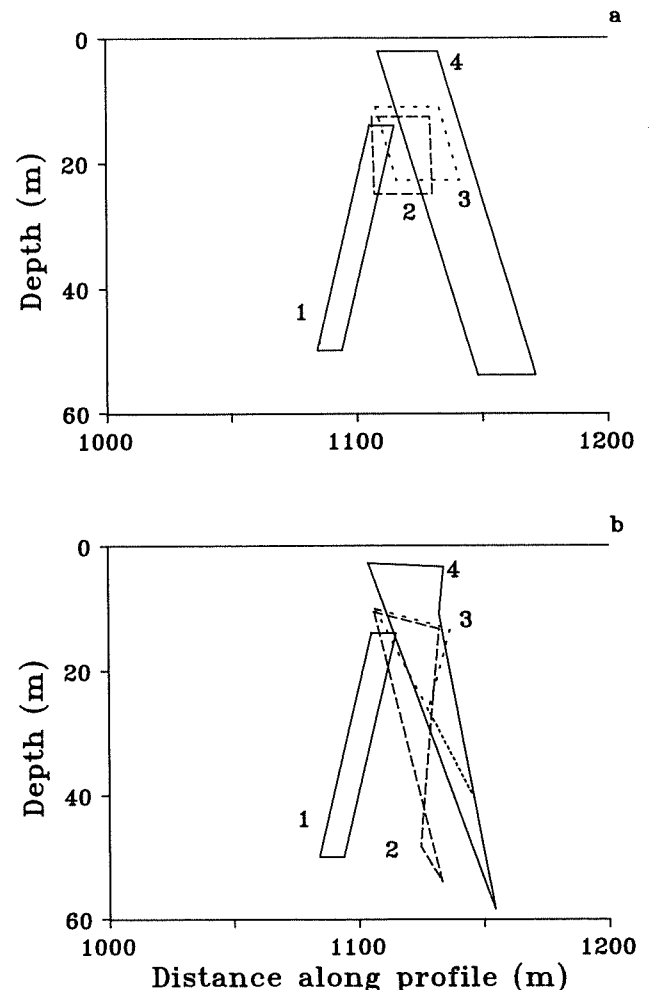


Figure 5 Progressive changes of the magnetised body produced by two different versions of the modelling program fitting the same trial dataset. (a) The output of the final version of the program restricted to fitting a dyke-shaped body to the data. (b) The results produced by an earlier version able to fit any four-cornered shape to the data. The bodies are numbered in sequence, with 1 representing the starting position. (4 does not represent the final model; only the situation after the fourth iteration out of several hundred.)

Figure 5a. Despite this quite severe restriction on the shape of the body, it was found that the fits produced by a dyke-shaped body for all the trial datasets were only slightly worse than for a general body.

Secondly, optional constraints were included. As a result of this modification, any combination of the parameters describing the geometry and magnetisation of the dyke could be varied in the final version of the program. For example, if it is known that the dyke outcrops at the surface, then the parameters describing the top surface of the dyke can be fixed, and the program instructed just to vary the bottom surface and magnetisation. Or, if the magnetisation is known to be induced, with no remanent contribution, the declination and inclination of the magnetisation can be fixed in the same direction as the main field, and the geometry of the dyke, along with the intensity of magnetisation, can be allowed to vary.

As well as these optional constraints, which can be applied during the running of the program, several "obvious" constraints were built into the program, such as the requirement that the bottom surface of the magnetised body should always lie below the top surface, and that the top surface should always be below the level at which the measurements were taken. This ability to create a program structure which could cope with both optional and built-in constraints, and which allowed these built-in constraints to be modified without undue difficulty, was due to the great flexibility of the simplex method.

Thirdly, a restart procedure was added to effect an escape mechanism from shallow local minima and allow the simplex to proceed towards a deeper minimum. If the simplex is regarded as a body rolling over a hypersurface and becoming trapped, for example, in a small depression on a plateau, then the restart procedure effectively deforms the shape of the simplex by a small random amount in order to push it out of the depression and set it into motion again. To give the user the choice of a potentially more severe restart, a second procedure was included which enabled the user to restart the optimisation process with a changed set of parameters. The optimisation process can then be directed towards any part of the parameter space, so allowing all possible models to be investigated.

With the above three modifications, the program is sufficiently flexible and robust to cope with virtually any situation. We now describe the application of the program to interpreting the Blairgowrie anomaly.

### 4.3. Geometry of the deep magnetic source of the Blairgowrie anomaly

The initial concern was to model the deep body producing the long wavelength component of Figure 3. Before this can be done, the effects of near-surface bodies have to be smoothed. This was done using a robust smoother (Tukey 1977) based on running medians.

It was also decided to remove from the profile the sharp peak at 8.6 km and the major trough between 10.4 and 11.5 km. These medium wavelength features are presumed to be generated by more local, shallow sources.

As the line of each fault to the immediate NW of Blairgowrie is virtually unaffected by topography, the faults must be close to vertical. The magnetised body producing the anomaly is probably bounded by two of these faults and so the dip of the dyke in the modelling program was fixed at 90°. The declination of magnetisation was also kept fixed at 35°W of N to lie along the line of the profile. Apart from these two constraints the minimisation process was allowed

**Table 1** The parameters describing the dimensions and magnetisations of the four bodies which produced the final model for the Blairgowrie anomaly shown in Figure 3

| Body | Horizontal position of each corner (km) | Depth of each corner (km) | Magnetisation: intensity, declination, inclination |
|------|---|---------------------------|--|
| 1    | 8.1                                     | 1.7                       | 235 nT   |
|      | 8.1                                     | 15.1                      | -35°   |
|      | 11.0                                    | 15.1                      | 101°   |
|      | 11.0                                    | 1.7                       |  |
| 2    | 8.5                                     | 0.01                      | 95 nT  |
|      | 8.5                                     | 1.7                       | -5°  |
|      | 9.1                                     | 1.7                       | 81°  |
|      | 9.1                                     | 0.12                      |  |
| 3    | 10.2                                    | 0.01                      | 115 nT   |
|      | 9.6                                     | 0.31                      | -5°  |
|      | 9.6                                     | 0.45                      | 70°  |
|      | 10.7                                    | 0.01                      |  |
| 4    | 11.2                                    | 0.05                      | 255 nT   |
|      | 9.1                                     | 0.66                      | -5°  |
|      | 9.1                                     | 0.77                      | -50°   |
|      | 11.6                                    | 0.05                      |  |

to vary all the other parameters describing the shape, size and magnetisation of the body. The declination of the main field was taken as -5°, and the inclination of the main field as 70° (positive downwards). The best fitting model had a residual sum of squares of  $3.03 \times 10^5 (\text{nT})^2$ . To achieve this fit, seven parameters were simultaneously and automatically adjusted by the program. These were: (i) the top, (ii) the base, (iii) the left-hand side and (iv) the width of the prism; (v) the intensity and (vi) the inclination of the magnetisation in the plane of the profile; (vii) the regional magnetic field level. The parameters of the best-fitting model for the deep body are listed in Table 1 as Body 1.

### 4.4. Bounds on the optimal body

The inherent ambiguity of geophysical inverse problems precludes quantification of the uncertainties in the recovered model parameters which have generated the best fit solutions. Nevertheless we employ a sensitivity analysis in order to investigate which parameters of our model are relatively well determined, and which are poorly determined. Having once established a best fit, we can again use optimisation techniques to investigate the range of models which fit the data adequately, although not quite as precisely as in our best fit solution. In practice, only a modest amount of extra FORTRAN coding is needed to achieve this analysis of model bounds using the earlier simplex method. We now use the residual sum of squares (RSS) as a constraint and seek to maximise or minimise individual model parameters (e.g. the depth to the base of the prism, or the inclination of the magnetisation) subject to the constraint that  $\text{RSS} < 1.05 \times \text{RSS}_{\text{opt}}$ , where  $\text{RSS}_{\text{opt}}$  is the residual sum of squares for the best-fitting model.

Application of this method to the range of prism shapes supported by the Blairgowrie total field measurements produces the results of Figure 6. The bounds on the location of the northern and southern edges of the body neatly enclose the mapped surface positions of the major faults in Figure 2. This comparison gives us confidence that the bounds on the depth to the upper surface are also realistic. The base of the magnetised prism remains poorly determined, despite the length of the measured profile.

#### 4.5. The shallower bodies

Once a satisfactory model had been produced for the long wavelength component of the Blairgowrie anomaly, an effort was made to interpret some of the more prominent medium wavelength features. The calculated anomaly for the best-fitting deep body listed as Body 1 in Table 1 was removed from the measured values along the profile. The most suitable interpretation of features close to the peak of the long wavelength component of the anomaly, between 8 and 13 km from the start of the profile, was found to involve three bodies. Unfortunately, the new modelling program can, at present, only deal with the anomaly due to a single magnetised body. Thus it cannot be applied to the medium wavelength features as the individual anomalies of these three bodies overlap to a significant extent, and so are not independent. Instead, the usual technique of trial and error using forward modelling was used. This proved a good test of how much of an improvement the addition of an

optimisation routine made to the modelling procedure. It took two days to arrive at a plausible model for the near-surface features, compared with the two computer runs to produce the best model of the deep body.

The final model for the medium wavelength features, combined with the best model for the deep body, is shown in Figure 3. The parameters describing each of these bodies are listed in Table 1. In producing the model for the medium wavelength features, it was assumed that the most southerly shallow body had vertical sides and extended down to the top surface of the deep body. This body is interpreted as a block uplifted close to the surface along a fault. This might correspond to the outcrop of serpentinite found 10 km along strike to the NE near Incheoch [NO 250 524].

The two other shallow bodies are interpreted as two andesitic lavas crossing survey line 4 half way along its length near Mains of Mause [NO 167 498], and dipping at approximately  $10^\circ$  to the SE (Fig. 2). Because the traditional modelling technique of trial and error was used, and because the spacing between measurements of 100 m was not selected for examining bodies of this size, the models for the near-surface bodies are not as accurate as the model for the deep body. In order to produce the negative anomaly on the northern flank of the main Blairgowrie anomaly the two lavas had to be given resultant magnetisations of opposite sign, as the directions listed in Table 1 show. This explanation requires that the more northerly lava is reversely magnetised. It was decided to continue the investigation by a palaeomagnetic study of the surface bodies in order to check the magnetisation directions derived from the modelling.

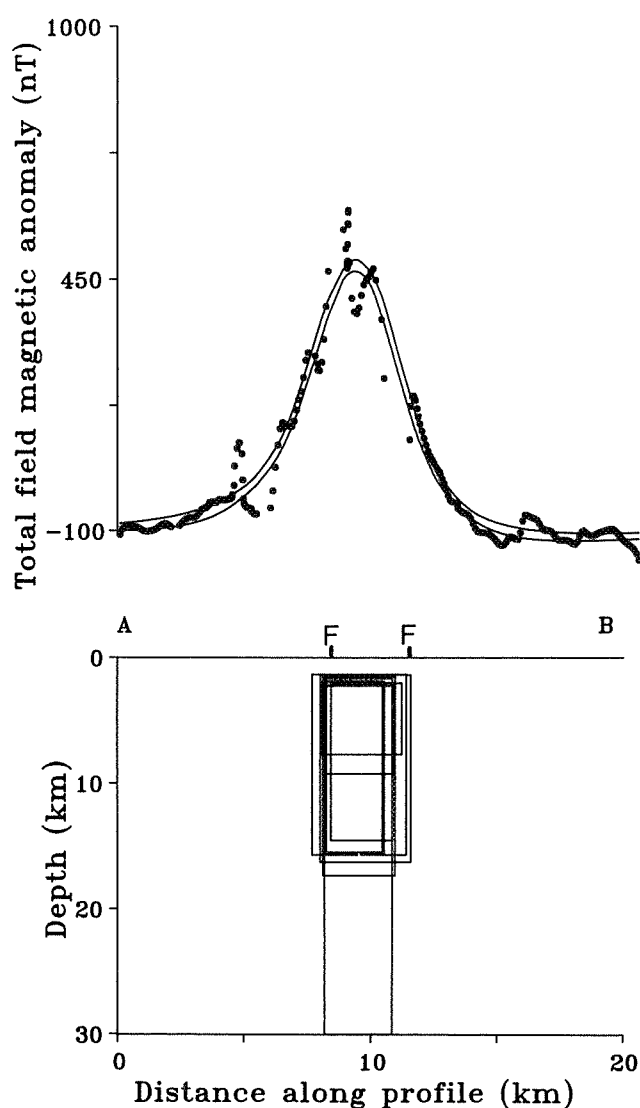


**Figure 6** The range of possible models for the long wavelength component of the Blairgowrie anomaly which are constrained to have a residual sum of squares within 5% of that of the best-fitting model, and which illustrate the most extreme positions of the four surfaces of the body allowed by this constraint. The circles correspond to the smoothed data considered to be the most suitable representation of the long wavelength component of the anomaly, and the two curves define the envelope within which the anomalies produced by this extreme range of blocks lie. Note the different vertical scale from Figure 3. The surface outcrops of two of the major faults of the region are denoted by the F symbols.

## 5. Palaeomagnetic investigation of surface magnetic bodies

### 5.1. Sample collection and measurement

Exposures of the three shallow bodies (2, 3 and 4 of Fig. 3) were visited and three orientated sample blocks collected at each locality. Rock cores one inch in diameter were later drilled from the blocks and cut into specimens 0.8 inches long for measurement. The lava samples were easy to subsample, but the highly shattered nature of two of the serpentinite blocks precluded drilling or sawing of the blocks. Instead, chips of the orientated rock surface were gently broken off for measurement.

Magnetic susceptibility was measured on an air-cored induction bridge and natural remanence directions and intensity were measured on either a Molspin fluxgate magnetometer, or, for the less strongly magnetic samples, on a 2G cryogenic magnetometer. Fisherian mean directions were calculated for each sample block and site means were derived by averaging sample block means (Table 2). Good remanence groupings were derived from all three sites. Table 2 also includes median values of both the natural remanent magnetisation (NRM) intensity and susceptibility for each site.

### 5.2. Demagnetisation studies

Thermal and alternating field partial demagnetisation studies were performed to test the natural remanence stability. Remanences were found to be stable and comprise predominantly single component magnetisations. The demagnetisation results are summarised in the orthogonal projection diagrams of Figure 7 for one specimen from each

**Table 2** Palaeomagnetic results

|              | No. of<br>samples | No. of<br>specimens | Mean NRM<br>declination | Mean NRM<br>inclination | Median<br>NRM<br>(mAm <sup>2</sup> kg <sup>-1</sup> ) | Median<br>susceptibility<br>( $\mu\text{m}^3\text{kg}^{-1}$ ) | Koenigsberger<br>ratio |
|--------------|-------------------|---------------------|-------------------------|-------------------------|---|---|------------------------|
| S. lava      | 3                 | 21                  | 243°                    | 40°                     | 0.27  | 4.3   | 1.7                    |
| N. lava      | 3                 | 15                  | 87°                     | -56°                    | 0.29  | 4.0   | 1.4                    |
| Serpentinite | 3                 | 11                  | 332°                    | 69°                     | 0.4   | 10  | 0.87                   |

of the three bodies. The projection azimuth has been chosen to coincide with the azimuth of our magnetic anomaly profile.

### 5.3. Comparison of palaeomagnetic remanence vectors and modelled magnetisations

All the rocks we measured were found to have Koenigsberger ratios (remanence divided by susceptibility times field) of about unity (Table 2). Hence their resultant magnetisations comprise roughly equal induced and remanent components and for a good match between modelled magnetisations and laboratory remanence measurements, the modelled magnetisations should lie about midway between the ambient geomagnetic field direction (a declination of -5° and an inclination of 70° at Blairgowrie) and the palaeomagnetic directions. This situation is indeed close to the pattern we found. In particular, the serpentinite samples all had steeply inclined palaeomagnetic remanences (Table 2), matching the almost vertical modelled magnetisations of both the most southerly shallow body and the deep body. Also, the Mains of Mause lavas unambiguously displayed the opposed polarities predicted by the modelling work, as can be seen by comparing parts a and b of Figure 7. In fact, the median values for the apparent palaeomagnetic inclination in the plane along the profile were 81° and -109° for the southern and northern lavas respectively. So, when these magnetisations are combined with an induced component of similar magnitude in the ambient field direction, there is remarkable agreement with the modelled values of the apparent, resultant inclination of 73° and -54° respectively. We can thus be confident that the medium wavelength features of our profile have been correctly attributed to these three shallow magnetic sources.

When remanence directions of the lavas are rotated back to the palaeohorizontal, a palaeomagnetic pole at 15° Lat. 308° Long. is derived which is very close to the Lower Devonian reference poles of Torsvik *et al.* (1990) in the vicinity of 0° Lat. and 320° Long. The Mains of Mause lavas, despite lying within the heart of the Highland Boundary Fault Zone, appear to have retained an excellent record of the ancient Devonian geomagnetic field.

## 6. Discussion

The long wavelength component of the Blairgowrie anomaly can be modelled in terms of a large magnetised body whose top surface is at a depth of approximately 2 km (Fig. 3). The geological nature of this body is open to debate. However, the occurrence of serpentinite along the whole Highland Boundary Fault Zone (Anderson 1946) and the disposition of a 500 foot wide serpentinite zone only 4 miles to the NE (Allen 1928), coupled with the strong magnetic properties of this type of rock (Piper 1978; Shive *et al.* 1988), suggest that the body could be made up of ultra-basic, metamorphic material, such as serpentinite, which has been brought up between the two major faults of the zone.

The Blairgowrie aeromagnetic anomaly stands proud from the flat aeromagnetic topography in its immediate vicinity (Fig. 1a), and is much more pronounced than the undulating anomalies further to the N and NE (Fig. 1a) associated with Caledonian granites and basic intrusions. Also, we found that the four-block model produced to account for our surface measurements fits the aeromagnetic data well. The aeromagnetic anomalies associated with the most extensive Scottish exposures of serpentinite, at the Ballantrae complex, are not dissimilar to the Blairgowrie anomaly. At Ballantrae they are somewhat stronger, reaching 800 nT in amplitude (Powell 1978; Stone & Smellie 1988).

As well as the aeromagnetic anomaly, there is a similarly shaped Bouguer gravity anomaly over the complex region of the Highland Boundary Fault Zone in Fig. 1 (Hipkin & Hussain 1981). The amplitude of this gravity anomaly is approximately 100 gu. using the equation for the gravity anomaly due to a two-dimensional prism (equation 2.49c, Telford *et al.* 1985), a density contrast of 25 kg m<sup>-3</sup> between the deep body in Figure 3 and the surrounding rocks would be required to produce an anomaly of this amplitude. This density contrast is very small, and hence does nothing to lessen the ambiguity in the possible composition of the body. At Ballantrae, a negative Bouguer anomaly with an amplitude of the order 100 gu is associated with the large aeromagnetic anomaly. Despite the opposite signs of the Bouguer anomalies at Blairgowrie and Ballantrae, they can both be modelled by a body only slightly different in density from the rocks in which they are embedded. This is in direct contrast to the very strong magnetic properties necessary to produce the aeromagnetic anomalies at both Blairgowrie and Ballantrae.

Our measurements of susceptibility and magnetic remanence from the three shallow bodies in Figure 3 satisfactorily account for the medium wavelength components of the Blairgowrie magnetic anomaly. The palaeomagnetic remanence intensity of the lavas is much stronger than that assumed for the two northerly blocks in the modelling. In retrospect, the dimensions of the modelled lavas could be considerably reduced and the magnetisation intensity correspondingly increased. The laboratory measurements of the serpentinite magnetic properties are also stronger than the modelled intensities for Bodies 1 and 2 in Table 1. In this case, the differences could suggest that serpentinite and basic/ultrabasic igneous rocks probably make up only a part of the modelled deep body, presumably in a similar manner to that of the Ballantrae complex.

Although the Blairgowrie anomaly is a very linear feature, allowing the profiles at Blairgowrie to be interpreted in terms of two-dimensional models, it ends abruptly at Dunkeld to the SW, and dies away at Glen Clova to the NE. If the proposed deep body of serpentinite was brought up between two major faults, the merging together of these two boundary faults could account for the termination of the anomaly at its two ends. The form of the anomaly also suggests that any continuation of the ultrabasics to the N or S must lie deeper than 13 km.



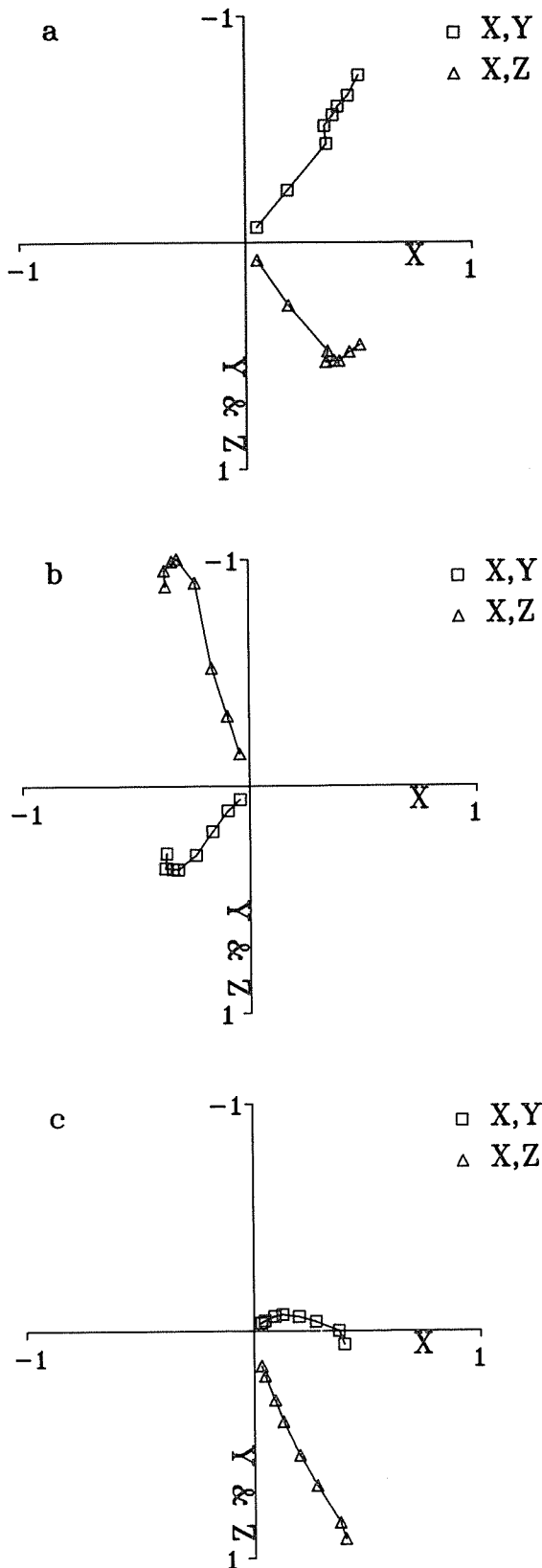


**Figure 7** Orthogonal projection diagrams showing the results of thermal demagnetisation of samples from (a) the southerly lava, (b) the northerly lava, and (c) the serpentinite (i.e. bodies 3, 4 and 2 in Fig. 3). The XY plane is the horizontal plane with X in the direction of the profile (corresponding to line AB in Fig. 2), and the XZ plane is the vertical plane along the profile. The values plotted represent the NRM, then demagnetisation steps of 100°C from 100°C to 600°C, and a final demagnetisation at 650°C. The projected remanent components have been normalised with respect to the intensity of the NRM.

Since our programming and modelling studies were completed, Marobhe (1990) has published an automated maximum gradient method of magnetic anomaly interpretation. While the simplex method is much less elegant than the linearised approach of Marobhe, it would appear to retain some advantages in the ease with which constraints can be added, and the facility for extension of the simplex method to estimate confidence bounds.

## 7. Conclusions

1. The use of an optimisation procedure, such as the Nelder and Mead simplex algorithm, greatly improves efficiency and quality of the modelling process for interpreting the total field magnetic anomaly profile across a two-dimensional structure.

2. The long wavelength component of the total field magnetic anomaly at Blairgowrie can be modelled in terms of a rectangular magnetised prism with approximate width and vertical extent of 3 km and 13 km respectively, and with a depth of 2 km to its top surface. The most likely composition of this body is a highly altered, ultra-basic rock.

3. The Mains of Mause lavas retain a record of two polarity states of the Lower Devonian geomagnetic field.

4. The deep, main source body of the Blairgowrie anomaly probably extends some 40 km from Dunkeld in the SW to Glen Clova in the NE, giving it a volume of roughly 1500 km<sup>3</sup>.

## 8. Acknowledgements

We are very grateful to I. B. Paterson and J. Mendum for advice about the geology around Blairgowrie and for suggestions for sampling localities, and to R. G. Hipkin for help with magnetic anomaly interpretation.

## 9. References

- Allen, D. A. 1928. The geology of the Highland Border from Tayside to Noranside. TRANS R SOC EDINBURGH LVI, 57–88.
- Anderson, J. G. C. 1946. The geology of the Highland Border: Stonehaven to Arran. TRANS R SOC EDINBURGH LXI, 479–515.
- Armstrong, M. & Paterson, I. B. 1970. *The Lower Old Red Sandstone of the Strathmore region*. Rep. No 70/12, Inst. Geol. Sci. 23pp. London: HMSO.
- BGS, 1981. 1 : 250000 Sheet 56°N 04°W, Tay–Forth (Aeromagnetic Anomaly), British Geological Survey.
- Gill, P. E., Murray, W. & Wright, M. H. 1981. *Practical optimization*. London: Academic Press.
- Heiland, C. A. 1940. *Geophysical exploration*. New York: Prentice-Hall.
- Hipkin, R. G. & Hussain, A. 1981. Regional Gravity Map of the British Isles, Northern Sheet, 1 : 625000, Univ. of Edinburgh.
- Marobhe, I. M. 1990. A versatile Turbo-Pascal program for optimization of magnetic anomalies caused by two-dimensional dike, prism, or slope models. COMPUT GEOSCI 16, 341–65.
- Nelder, J. A. & Mead, R. 1965. A simplex method for function minimization. COMPUT J 7, 308–13.
- Parasnis, D. S. 1979. *Principles of applied geophysics*. 3rd Edn. London: Chapman and Hall.
- Piper, J. D. A. 1978. Palaeomagnetism of the Southern Uplands block in Ordovician times. SCOTT J GEOL 14, 93–107.
- Powell, D. W. 1978. Geology of a continental margin 3: gravity and magnetic anomaly interpretation of the Girvan-Ballantrae district. In Bowes, D. R. & Leake, B. E. (eds) *Crustal evolution in northwestern Britain and adjacent regions*, 151–62. GEOL J SPEC ISS No 10.
- Press, W. H., Flannery, B. P., Teukolsky, S. A. & Vetterling, W. T. 1986. *Numerical recipes: the art of scientific computing*. Cambridge: Cambridge University Press.

- Shive, P. N., Frost, B. R. & Peretti, A., 1988. The magnetic properties of metaperidotite rocks as a function of metamorphic grade: implications for crustal magnetic anomalies. *J GEOPHYS RES* **93**, B10, 12187–95.
- Smith, R. A., 1959. Some depth formulae for local magnetic and gravity anomalies. *GEOPHYS PROSP* **7**, 55–63.
- Stone, P. & Smellie, J. L. 1988. Classic areas of British Geology: the Ballantrae area: a description of the solid geology of parts of 1:25000 sheets NX08, 18 and 19. London: HMSO for British Geological Survey.
- Telford, W. M., Geldard, L. P., Sheriff, R. E. & Keys, D. A. 1985. *Applied geophysics*. Cambridge: Cambridge University Press.
- Torsvik, T. H., Smethurst, M. A., Briden, J. C., and Sturt, B. A. 1990. A review of Palaeozoic palaeomagnetic data from Europe and their palaeogeographical implications. In McKerrow, W. S. & Scotese, C. R. (eds), *Palaeozoic palaeogeography and biogeography*. *GEOL SOC MEM* **12**, 25–41.
- Tukey, J. W. 1977. *Exploratory data analysis*. Reading, Mass: Addison-Wesley.

---

C. G. FARQUHARSON and R. THOMPSON, Department of Geology and Geophysics, The University of Edinburgh, Edinburgh EH9 3JW, U.K.

MS received 27 September 1990. Accepted for publication 11 November 1991.